

Crackling noise in paper peeling

L.I. Salmi¹, J.M. Pulakka¹, J. Rosti¹, M.J. Aalava^{1,2}, and K.J. Niskanen³¹Helsinki University of Technology, Laboratory of Physics,

P.O. Box 1100, FIN-02015 HUT, Finland

²SMC-INFM, Dipartimento di Fisica, Università "La Sapienza",

P.le A. Moro 2 00185 Roma, Italy and

³Finnish Pulp and Paper Research Institute,

P.O. Box 51, FIN-02151 Espoo, Finland

Abstract

Aoustic emission or crackling noise is measured from an experiment on splitting or peeling of paper. The energy of the events follows a power-law, with an exponent 1.8 ± 0.2 . The event intervals have a wide range, but superposed on scale-free statistics there is a time-scale, related to the typical spatial scale of the microstructure (a bond between two fibers). Since the peeling takes place via steady-state crack propagation, correlations can be studied with ease and shown to exist in the series of acoustic events.

PACS numbers: 62.20.Mk, 05.40.-a, 81.40.Np

There are several experimental signatures of power-law statistics, or scale-invariance, in fracture. One interesting case is acoustic emission (AE), which is produced by the release of small quantities of elastic energy during the failure of an inhomogeneous sample, and is an example of the phenomenon of "crackling noise", met in many kinds of systems in physics [1, 2]. This can result in analogies of the Gutenberg-Richter's and Omori's laws for earthquakes [3, 4, 5, 6, 7]. These are experimental observations; the former relates the probability (for earthquakes or AE) of an event $P(E)$ to the energy or magnitude of the event E by an exponent β . Correspondingly, the latter binds by an exponent α the waiting time t between the events and their probability $P(t)$. Very often these laws are witnessed simultaneously in both microfracturing and earthquakes [8]. The origins of both the power-laws are mostly unknown and the same holds also for the possible connection between these.

The common idea about material failure is based on a critical defect: the sample fails catastrophically once the local strength, that follows from among others the size of the flaw, is exceeded. The observation of AE implies often that microscopic damage is being created, contrary to one, single catastrophic crack growth event. One consequence is that, in analogy to earthquakes again, the idea of predictability becomes of interest. This is due to the precursors to final failure that could be diagnosed by AE. In general terms it is of fundamental materials science and statistical physics interest that universal or critical fracture behavior should exist in the presence of varying material properties, like anisotropy, related to the shape of the stress-field close to microcracks or a notch, or to e.g. asymmetric disorder [9]. Any power-laws in AE or crackling noise should originate from a basic, fundamental mechanism, in spite of such complications.

One particularly inviting proposal is to follow the passage of a crack front through a quasi two-dimensional sample, which can be realized e.g. in a weak interface between two three-dimensional elastic plates [10, 11]. This scenario has the advantage, over say ordinary tensile tests, that the crack propagation takes place in a steady-state in contrast to most other experiments of fracture. In plexiglass, the front may be self-affine, and a roughness exponent close to 0.6 has been measured, which is intriguing given that the advancement takes place in avalanche-like events [12]. The theoretical understanding of the phenomenon is based on numerical models and on stochastic equations for the crack line dynamics. These have so far not been able to account for most of the observed features, nor is there any

understanding of whether the roughening could be expected to be "universal".

In this work we look at the statistics of fracture AE in a set-up that mimics such line dynamics in ordinary paper by peeling a sheet into two, as a crack advances through it (Figs. 1 and 2). We obtain that the energy of AE events scales as a power-law, like in tensile tests, which produce analogies of both the Gutenberg-Richter and Omori's laws. This takes place with a novel exponent which is much larger than those usually met in fracture AE. The temporal statistics exhibit a wide spectrum of intervals between the events. Translated into the average distance that the fracture line propagates we show below that there is a typical scale, related to the size of a fiber-to-fiber bond. Rupture processes often involve time-dependence, but at least for low strain rates the structural scale stays the same. The dynamics of the peeling line is most likely quasi-one-dimensional. That is, due to the thinness of a sheet of a paper the stress field is not able to penetrate into the intact paper so as to give rise to two "scalefree" length scales [13]. We also compare to other kind of AE data for the same materials, demonstrating that for localized fracture, the β -exponent is much larger, and that in a tensile test values met before can be obtained [7]. Such experimental data should be useful to formulate and test microscopic fracture models.

In the case of paper, Yamuchi made pioneering acoustic emission measurements [14], with the claim that fiber and bond breakages can be distinguished in the amplitude histogram of the signal. The idea of basic scales should be contrasted with Fig. 2 that introduces the crack advancement scenario. Due to the nature of the set-up, the stress-field is expected to be cut-off quickly (in some models exponentially) with increasing distance from the average crack line position. Thus the individual events, interpreted in terms of the area over which the "avalanche" passes, are in practice one-dimensional. Of course, the crack can fluctuate on very small scales in the z-direction, perpendicular to the sheet.

With intact samples in a tensile test the strength depends on weak spot statistics. In practice some existing weak region often launches the crack growth, and after that rupture becomes mainly a local problem. Naturally, if a sizeable initial (edge or center) notch is applied, the fracture process focuses in the so-called fracture process zone, FPZ, around the crack-tip (for paper, the characteristic dimension of FPZ is upto 5 mm, typically). Since fracture can happen in a diffuse or in such a localized way one might see two separate statistics related to these processes, and distinguish two regimes. These would be the pre-fracture phase, when behavior is nearly elastic and cracking or damage disperse and the

second part taking place after and at the stress maximum. During this regime a single crack is propagating and the failures concentrate in the FPZ, the vicinity of the crack-tip.

In the presence of disorder the fracture can be an irregular process of elementary rupture events separated by interarrival or waiting times, and spread out geometrically in the sample. The variety of theoretical or computer models available differ in the level and details of load resharing after microfailures [15]. The events in such studies consist of single spring-like breakages, with a varying number of those elementary breakages within one coherent event. In the case the fracture takes place via the avalanche-like dynamics, 2d computer simulations indicate a β -value of 1.7 [16]. Also, $\beta = 0.94 \pm 0.20$ was reported in a simulation of hydraulic fracture [17]. All such studies do not apply to the peel-experiment at hand, i.e. there are no theoretical results pertaining to the possible AE statistics in our case.

Acoustic emission as such is a well-known technique to monitor fracture in e.g. composites. The rapid release of elastic energy can be observed by ultrasonic sensors [18], with little influence on the actual fracture process. The peel-in-nip method to split paper is based on the nip between two rolls rotating synchronously (Fig. 1). The front end of the sample is attached to both the rolls by tape and then the cylinders are reeled to initiate the peeling. Then the cleavage proceeds based on an equilibrium of three supporting forces. The peeling takes place near the nip so that angle between the planes of the halves is close to π and the actual value has a slight dependence on the particular kind of paper. The test produces very large fracture surfaces; over 100 m m^2 compared to a typical area 1 m m^2 in standard tensile tests. Paper is a fibrous material, such that the fibers form interpenetrating layers. In standard tests the fibers are loaded mostly in-plane, and several microscopic failure mechanisms co-exist (bond or fiber breakages, fiber pull-out). The fracture line separating the intact part and the separated halves is continuous, however the paper structure is discrete on scales below the fiber length. Thus some bond dimension related cross-over in any distribution (energy or intervals of events, or durations) is possible. Figure 3 demonstrates a typical test: note both that there is a maximum scale for interarrival times, and that, of course, the AE event size has no trend during the test.

We used two sets of handsheets, paper made in a standard laboratory mould from standard mechanical pulp. Typical tensile strength is 3 kN/m and strain at break 2%. One control parameter used is reining, or beating the pulp which makes the fibers more flexible and more fibrillated. Due to that the resulting paper is more uniform and becomes thus

stronger. Contrary to industrial paper the fiber orientation is uniform. We had a set of handsheets with six different rolling levels. Small (length 70 mm, width 15 mm) sample strips were used to reduce the elastic energy often leading on catastrophic crack growth, in ordinary tensile laboratory tests performed for comparisons.

During the experiment we acquire bipolar acoustic amplitudes simultaneously on two channels by piezocrystal sensors (Physical Acoustic Corporation R15 transducers, resonant frequency 150 kHz) as a function of time. In addition the force of peel-in-nip or tensile test was measured, typical values being a few tens of Newtons depending on the thickness and rolling friction of the grade of paper tested (in Fig. 3 about 90 N, with a variability of about 10 N). In tensile tests the two transducers were attached directly to paper and no coupling agent was used. Each channel has 12-bit resolution and a sampling rate of 400 000/s. The transmission time from event origin to sensors is order of 5 μ s. The acoustic channels were first fed through custom-made amplifiers, and after that held using sample-and-hold circuit. The shape of AE pulses can change and attenuate during transmission, but the effect should have only minor effect to our analysis. The acoustic time-series are reformatted online by thresholding, by the detection of continuous and coherent events, and by the calculation of event energy E , the sum of squared amplitudes within the event. Events are separated by silent (i.e. amplitude below threshold level) waiting intervals. We do not interpret the waveforms of the events but analyse the data in the statistical sense. The energy span is estimated to be about 1 μ J to 1 mJ; recall that the energy released ends up as heat eventually. In general the energy of the event is expected to be proportional to the damaged area corresponding to the event [19] and to the stress in that area.

The energy statistics shows that acoustic events obey a Gutenberg-Richter-like power-law for the peel-in-nip test (figure 4) with the value $\beta = 1.8 \pm 0.2$. The figure provides as a comparison the energy data from an ordinary tensile test: the exponent $\beta = 1.2 \pm 0.1$, in reasonable agreement with earlier such experimental values. These can also be compared to the value from a tensile test with a large initial notch, resulting in the exponent $\beta = 1.7 \pm 0.2$. Note that the peel-in-nip case presents some slight curvature. The difference in the exponent between this data and the tensile-with-notch appears us to be statistically reliable, in spite of the error bars. Notice that as is usual in an AE test the energy scale can not be calibrated quantitatively.

The different β -values imply that there are scale-free behaviors in both tensile and peeling

fracture, in the same material. Distributed damage all over the sample and microcrack coalescence, as in a tensile test, produces a small value for β . Such failures take place at weak spots with high local stresses. Any microscopic breaking stresses (fibers, bonds) will have bounded distributions (e.g. Gaussian), so the power-law distribution of energy implies that the number of elements (i.e. size) of rupture events has to vary in power-law manner. In the peel-in-nip test (and also with tensile samples with a large notch) the process reflects a more localized failure, but still scales as a power-law albeit with a much higher exponent. In the peeling experiment, most likely the dynamics is one-dimensional – the essential variation in the area covered by events, corresponding to the energy takes place along the crack line but not into the sheet, in the planar direction.

The variation in the exponents is analogous to the work by Lockner et al., on fracture and crack growth in granite [6]. They observed energy scalings with $\beta = 1.2$ to 2.3 , due to a setup that allowed to follow the variation of \dot{U} during the fracture. In that context it was suggested already earlier, by a model, that β should drop at maximum stress [20]. In addition the exponent was expected to recover after the start of crack propagation, as was seen qualitatively in the experiments of Lockner et al: β dropped from a value above 2 to near 1.2 at maximum stress, and recovered back to a value of 1.7.

The waiting time distribution in tensile tests often results in a distinct power-law [7]. With a large notch there is some scattering from pure scaling behavior. In both cases the exponent β is close to 1.0 (figure 5). The peel-in-nip experiment diverges clearly from such an ideal dependence in the time slot 10–500 ms. The fracturing takes place in a steady-state, but such that maximum waiting times take into account that the crack line has minimum velocity, imposed by the angular velocity of the rolls. The values reported in literature are without exception in the proximity of unity. For instance, in a creep experiment with a cellular glass material Mori's and Gutenberg-Richter laws were observed, with the values for $\beta = 1.3$ and $\beta = 1.5$ [21]. In AE experiments with ice $\beta = 1.0$ to 0.3 and $\beta = 1.3$ [22]. These should be different from the peeling set-up, where the events by force take place at or very close to the crack line. Given $\beta \approx 1$ the mechanism producing the scaling in all these might presumably be universal.

In order to study the origin of the typical scale in waiting time distribution, we did peel-in-nip experiments with various strain rates. We observed that the position of the "leap length" plateau shifts such that the length scale, interpreted as the distance that the fracture line

advances in a time corresponding to the position of the plateau, stays roughly constant. It is located between 1 mm and 50 mm, corresponding to a typical fiber width and fiber-to-fiber bond scale in paper. For a strain rate (500mm/m in) the leap plateau disappears. This may originate from strain at the wire pulling the rolls or inertia of the rolls, or the elastic energy stored into strained part of the sample. Without scaling the initial and final parts of the distributions overlap, which implies the presence of other effects related to the fast and slow time scales.

It is interesting to note that the Gutenberg-Richter exponents are close in tensile tests with notch and peel-in-nip tests and that the Omori exponent has close value in tensile and tensile with notch tests. These experimental findings underline that these two power-laws are produced by separate mechanisms. In particular it is possible to distort the energy scaling, only.

For short enough time windows the fracture line may advance in a correlated fashion. This is demonstrated in Fig. 6. One observes that large events, in terms of energy, are inter-correlated and more likely to follow each other than if the signal was completely random. The natural interpretation is that stronger crack line pinning is overcome in a correlated fashion, so that the consecutive events bear signatures of the energy stored due to the constant load rate, during periods of no acoustic activity. One can also study the autocorrelation functions (since the signal is stationary). This results in a similar picture, in that the signal is correlated up to a timespan which reaches about 0.05 s (depending on the straining rate), as depicted in Fig. 7. Note that for the slower rate the correlations extend further. The reference cases are artificial signals using a randomized sequence of (exactly the same) events and intervals. We also attempted to correlate the AE data with the force signal of the tensile testing machine; unfortunately it became apparent that the effective force at the crack line is masked by the two separate sheet halves that transmit it from the rolls. In particular no direct correlation between $E(t)$ and $F(t)$ could be detected. The time series as such exhibited $1/f$ noise, with an exponent close but below unity.

To conclude we have made experimental observations of acoustic emission in paper peeling. The set-up is such that steady-state crack propagation across a quasi-two dimensional material can be followed. The main discoveries are a power-law for the energies of the acoustic events, in spite of the fact that the process is confined to an almost one-dimensional geometry, and for the event waiting time statistics. The former supports some earlier ob-

servations, together with the tensile tests, that a strong localization of the fracture process produces scalefree statistics with a large exponent. The latter shows an intriguing deviation from a power-law, which seemingly can be attributed to the microstructure of paper.

- [1] J.P. Sethna, K.A. Dahmen, and C.R. Myers, *Nature* (London) 410, 242 (2001).
- [2] Scalefree cracks are discussed in: E. Bouchaud, *J. Phys. Cond. Mat.* 9, 4319 (1997).
- [3] A. Guarino, A. Garcimartín, and S. Ciliberto, *Eur. Phys. J. B* 6, 13 (1998); A. Garcimartín et al., *Phys. Rev. Lett* 79, 3202 (1997).
- [4] L.C. Krysac and J.D. Mays, *Phys. Rev. Lett.* 81, 4428 (1998).
- [5] A. Petri et al., *Phys. Rev. Lett* 73, 3423 (1994).
- [6] D.A. Lockner et al., *Nature* 350, 39 (1991).
- [7] L.I. Salmi, A.I. Tolvanen, and M.J. Alava, *Phys. Rev. Lett.* 89, 185503 (2002).
- [8] J.B. Rundle, S. Gross, W. Klein, C. Ferguson, D.L. Turcotte, *Tectonophysics* 277, 147 (1997).
- [9] J. Fineberg and M. Marder, *Physics Reports* 313, 1-108 (1999).
- [10] e.g. T. Halpin-Healy and Y.-C. Zhang, *Phys. Rep.* 254, 215 (1995).
- [11] S. Ramakrishnan, D. Ertas, and D.S. Fisher, *Phys. Rev. Lett.* 79, 873 (1997).
- [12] J. Schmittbuhl and K.J.M. Luy, *Phys. Rev. Lett.* 78, 3888 (1997); A. Delaplace, J. Schmittbuhl, and K.M. Luy, *Phys. Rev. E* 60, 1337 (1999). K.J.M. Luy, et al., *Int. J. Fract.* 121, 9 (2003).
- [13] S. Zapperi, H.J. Herrmann, and S. Roux, *Eur. Phys. J. B* 17, 131 (2000); Åström, M. Alava, and J. Timonen, *Phys. Rev. E* 62, 2878 (2000); M.J. Alava and S. Zapperi, *Phys. Rev. Lett.* 92, 049601 (2004).
- [14] T. Yamachi, S. Okumura, N. Noguchi, *Journal of Pulp and Paper Science* 16, (1990).
- [15] P.K. Nukala, S. Simunovic, and S. Zapperi, *J. Stat. Mech. Theo. Expt.*, P08001 (2004).
- [16] M. Minozzi, G. Caldarelli, L. Pietronero, and S. Zapperi, *Eur. Phys. J. B* 36, 203 (2003).
- [17] F. Tschichholz and H.J. Herrmann, *Phys. Rev. E* 51, 1961 (1995).
- [18] H. Corte, et al., in *The Role of Fundamental Research in Paper Making*, Ed. J. Brander, Mech. Eng. Publ. Ltd., (London, 1983), pp 571-584.
- [19] M.V. Lysak, *Eng. Fract. Mech.* 55 443, (1996).
- [20] J.D. Weeks, D.A. Lockner, and J.D. Byerlee, *Bull. Seism. Soc. Am.* 68, 333-341 (1978).
- [21] C. Maes, et al., *Phys. Rev. B* 57, (1998).

FIG . 1: Photograph of the peel-in-nip device, roll diameter is 80mm .

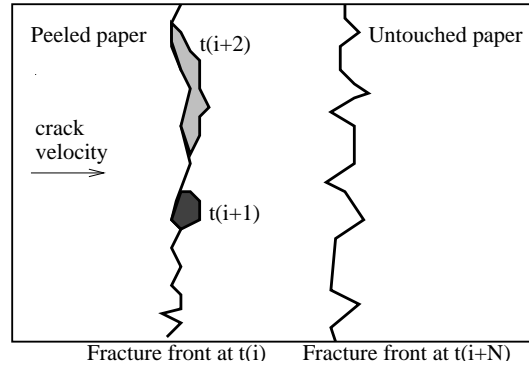


FIG . 2: Fracture propagation schematics in the peel-in-nip test.

[22] J. Weiss, J.R. Grasso, and P. Martin, Proc. 6th Int. Conf. on AE/M S in Geol. Struct. & Mat., 1996, 583-595, Trans Tech Publications, (Clausthal-Zellerfeld).

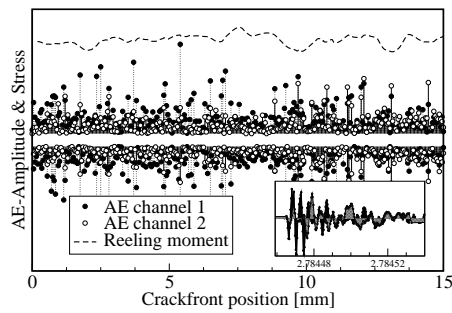


FIG . 3: Example of the data in peel-in-nip test. Both the AE channels, and the force or reeling moment signals are included. The former is in arbitrary units, for the latter see text.

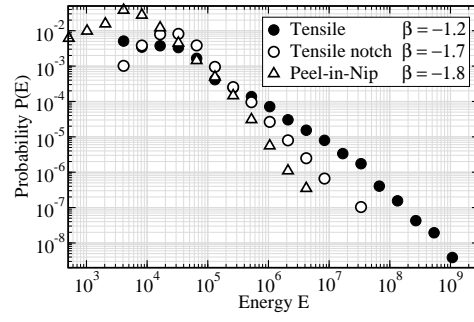


FIG . 4: Event energy distributions for the peel fracture and comparisons.

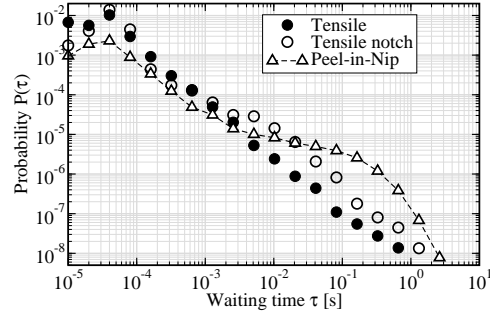


FIG . 5: Event interarrival time distributions for the same cases as in the previous figure.

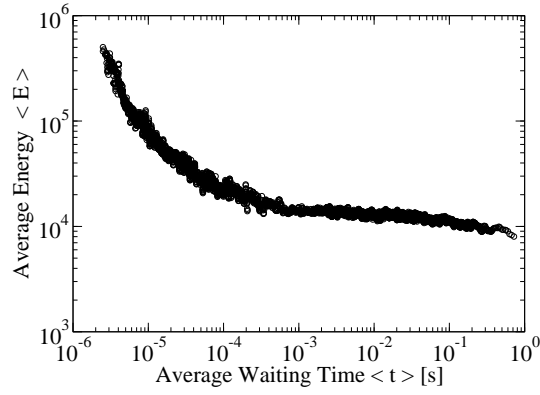


FIG . 6: Average energy (arbitrary units) in a window of twenty consecutive events, vs. the average waiting time in the same, for the peel-in-nip test.

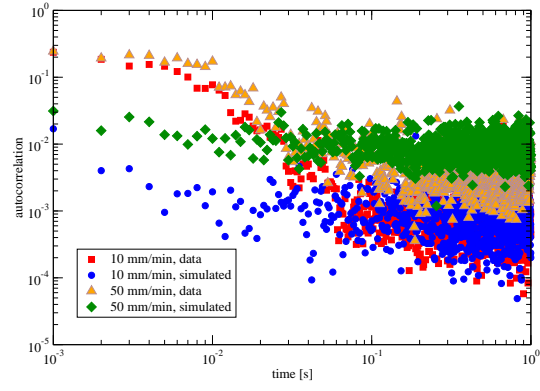


FIG . 7: Autocorrelations of the AE signal for two strain rates. As a comparison, a randomize signal is presented for both cases (see text).

This figure "R.jpg" is available in "jpg" format from:

<http://arxiv.org/ps/cond-mat/0601238v1>